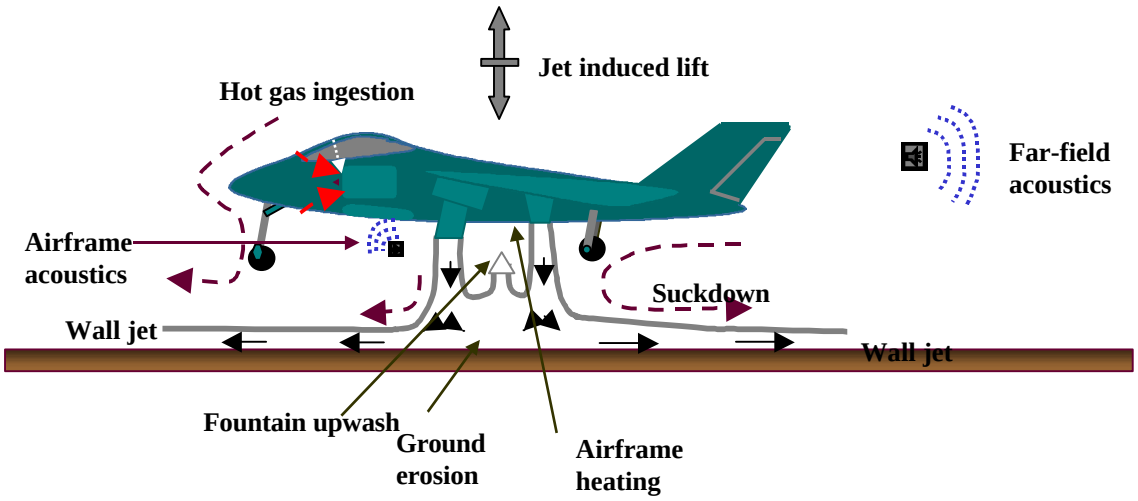

Fig. 1 - Flowfield created by the propulsion system around a STOVL aircraft.

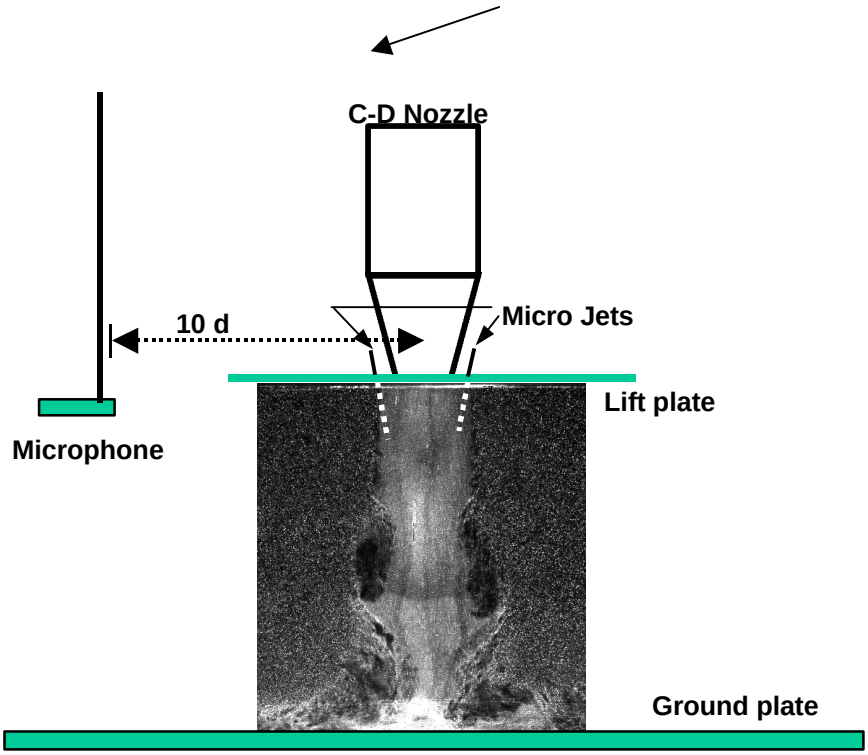

Fig. 2 - Schematic of the experimental arrangement.

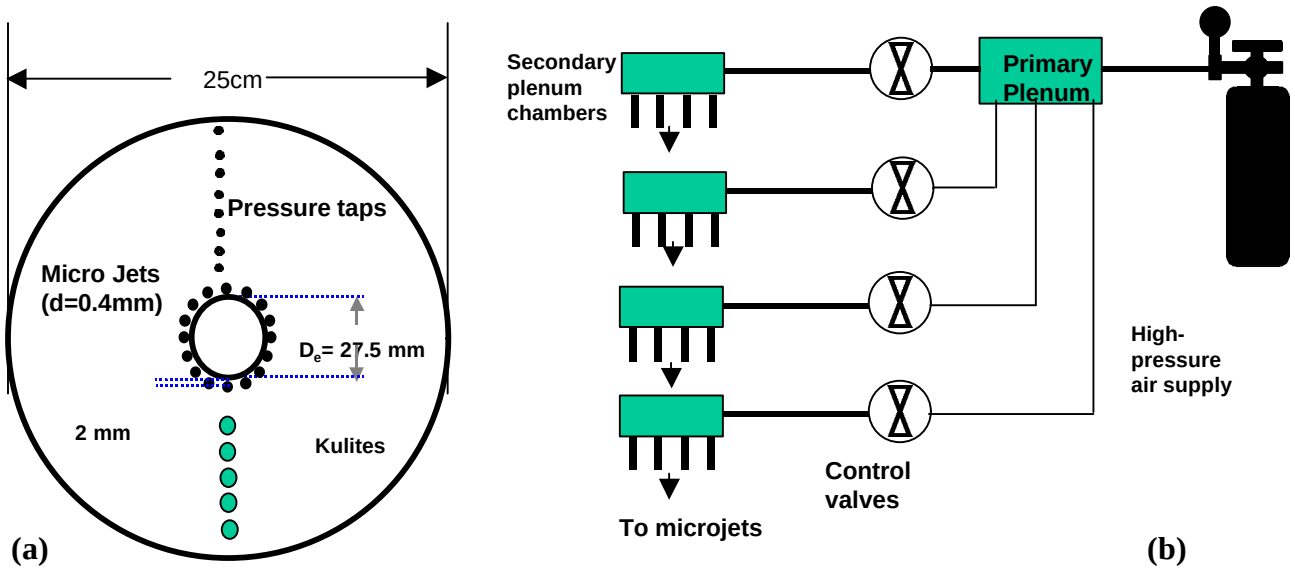

Fig. - 3. Microjet control hardware. a) Microjet locations on lift plate; b) Microjet air supply.

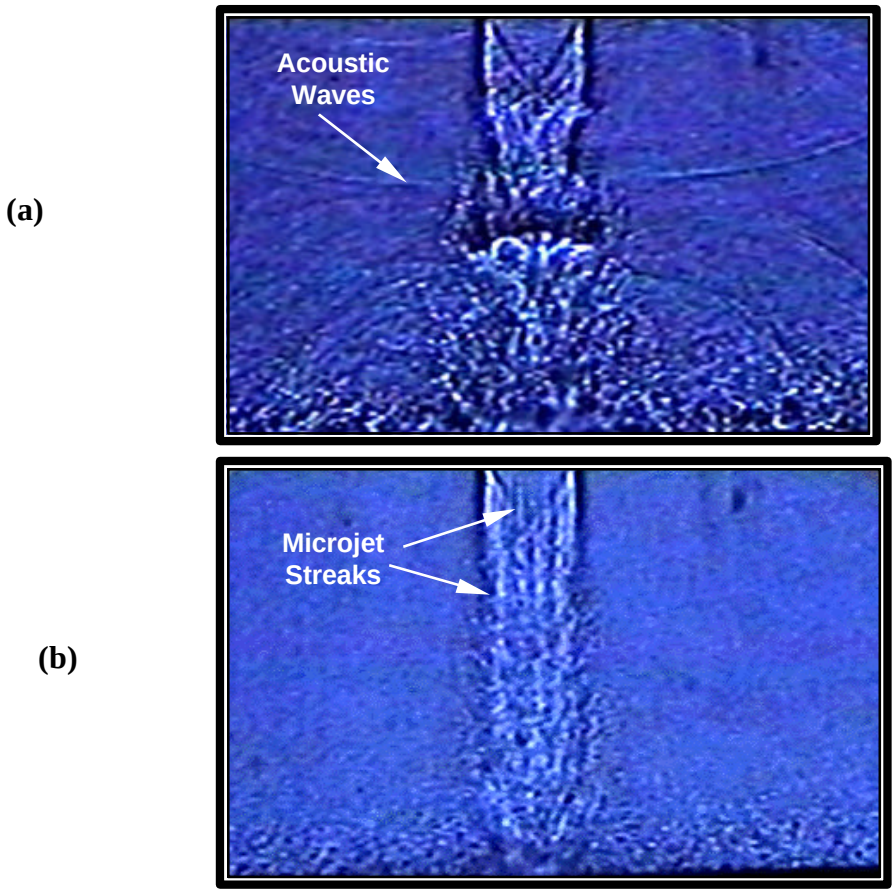

Fig. 4 - Instantaneous shadowgraph images, NPR = 3.7, h/d = 4.5.
a) No control; b) With microjet control.

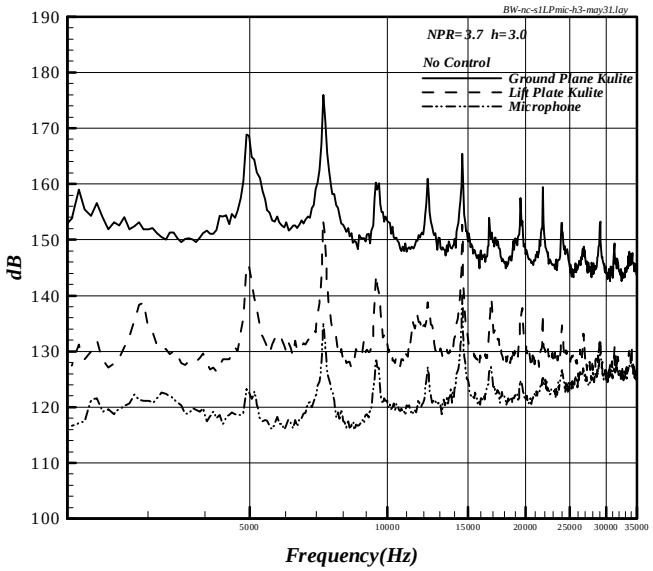

Fig. 5 - Unsteady surface pressure and microphone spectra for NPR = 3.7, h/d = 3.

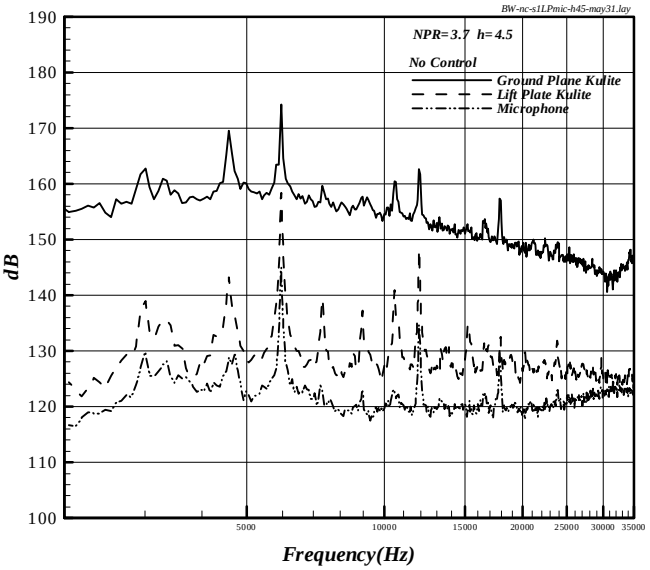

Fig. 6 - Unsteady surface pressure and microphone spectra for NPR = 3.7, h/d = 4.5

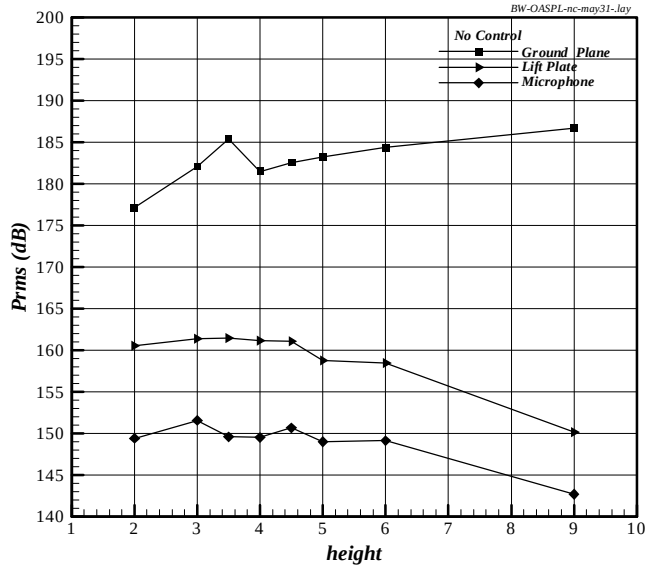

Fig. 7 – Fluctuating pressure intensities for NPR = 3.7, h/d=3.5

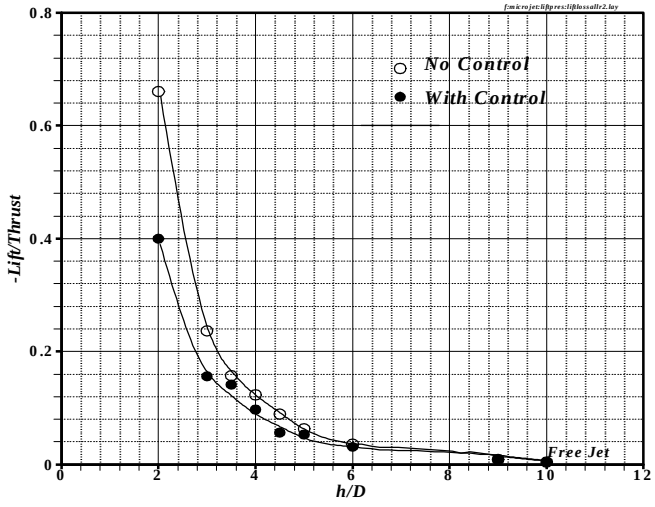

Fig. 8 - Lift loss variation with ground plane distance, with and without control;.NPR=3.7.

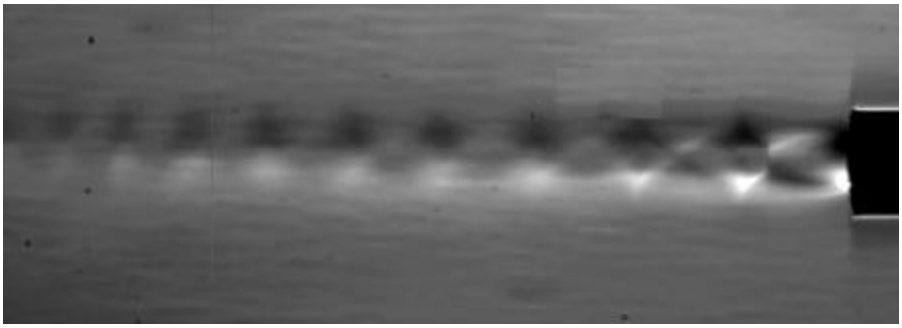

Fig. 9 - Schlieren image of a supersonic microjet issuing from a 400 micron nozzle, P_0 ~ 110 Psia.

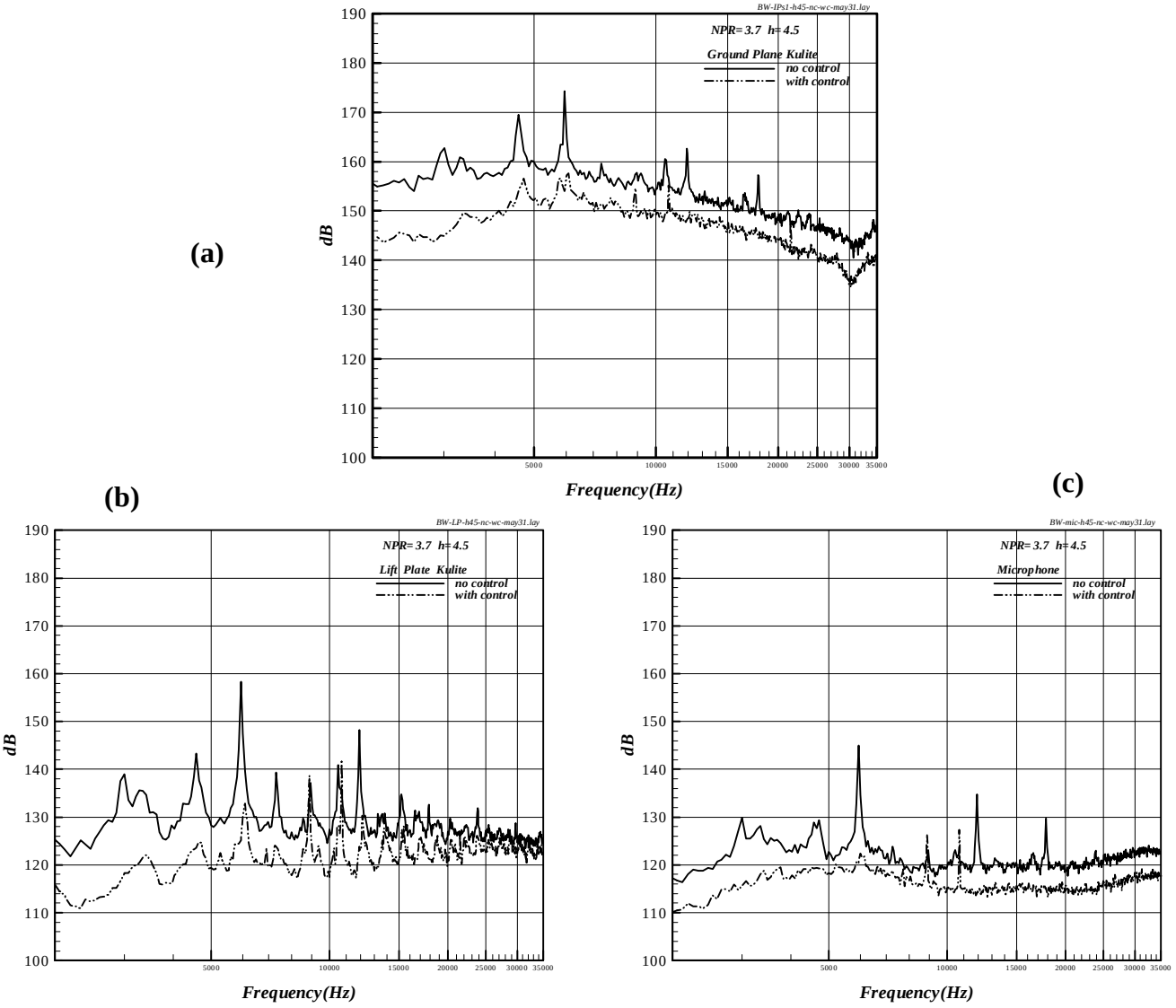

Fig. **10** - Unsteady pressure and microphone spectra with and without control, NPR=3.7, h/d=4.5. a) Ground Plane; b) Lift plate; c) Microphone.

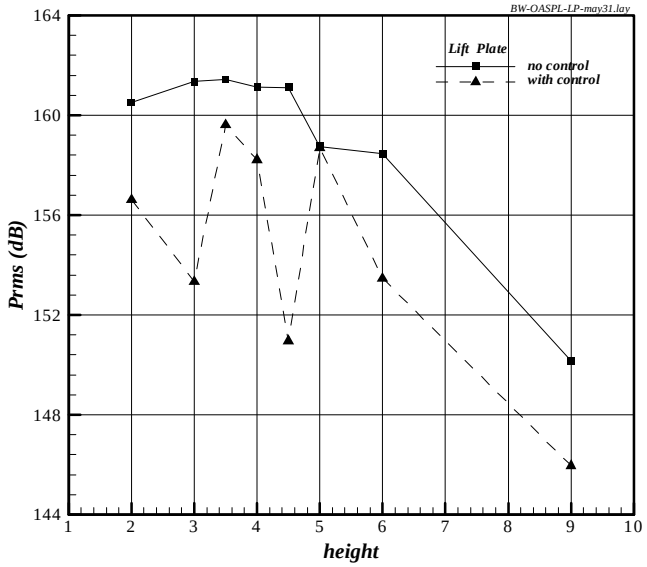

Fig. 11 - Fluctuating pressure intensities on the lift plate, with and without control. NPR = 3.7

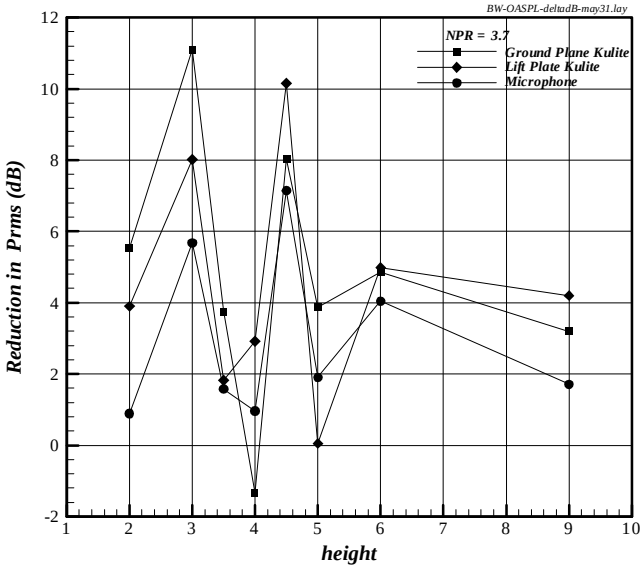

Fig. 12 – Reduction in fluctuating pressure intensities. NPR = 3.7

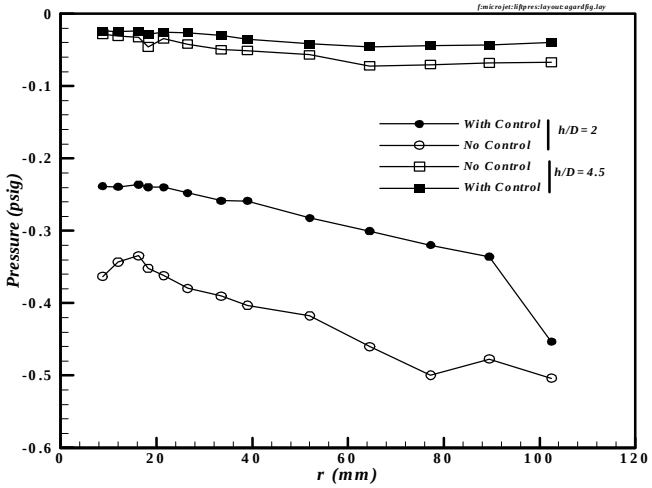

Fig. 13 - Mean Pressure distribution on the lift plate, with and without control at h/d = 2 and 4.5.

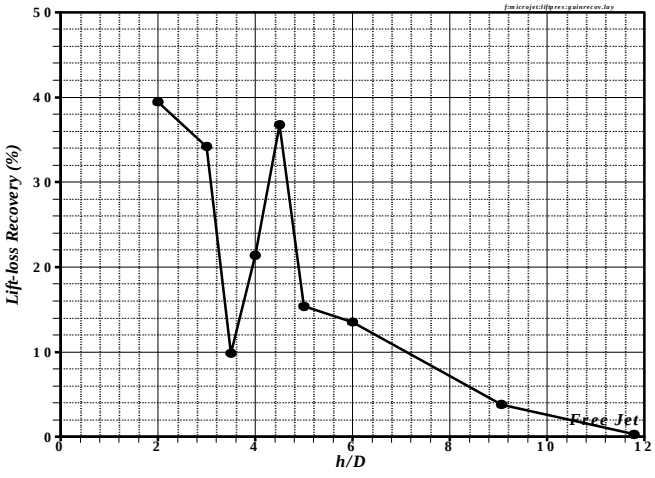

Fig. 14 - Lift loss recovery variation as a function of ground plane distance.